Conformational Stability from Temperature-Dependent FT-IR Spectra of Liquid Xenon Solutions, ab Initio Calculations, and r_0 Parameters for Methylhydrazine[†,‡]

James R. Durig,*[,§] Todor K. Gounev,[§] Chao Zheng,[§] Armen Choulakian,[§] and V. N. Verma[||]

Departments of Chemistry, University of Missouri−Kansas City, Kansas City, Missouri 64110, and University of Guyana, Georgetown, Guyana

Received: June 26, 2001; In Final Form: October 3, 2001

Variable-temperature (−55 to −100 °C) studies of the infrared spectra (3500−400 cm^{-1}) of methylhydrazine, CH_3NHNH_2, dissolved in liquid xenon have been recorded. From these data the enthalpy difference has been determined to be 323 ± 30 cm^{-1} (3.86 ± 0.36 kJ/mol) with the *inner* conformer (methyl group staggered and between the two hydrogens of the NH_2 group) the more stable rotamer. A complete vibrational assignment is presented for the inner conformer, and several of the fundamentals of the outer conformer have been assigned. These assignments are consistent with the predicted wavenumbers obtained from ab initio MP2/6-31G(d) calculations utilizing three scaling factors. The optimized geometries, conformational stabilities, harmonic force fields, infrared intensities, Raman activities, and depolarization ratios have been obtained from RHF/6-31G(d) and/or MP2/6-31G(d) ab initio calculations. Hybrid density functional theory (DFT) calculations to obtain the structural parameters and conformational stability by the B3LYP method were also carried out. These quantities are compared to the corresponding experimental quantities when appropriate. Additionally conformational stabilities and structural parameters have also been predicted from MP2 level calculations with full electron correlation with 6-311+G(d,p) and 6-311+G(2d,2p) basis sets. The r_0 structural parameters have been obtained from a combination of the previously reported microwave rotational constants and ab initio MP2/6-311+G(d,p) predicted parameters. The results are compared to some corresponding quantities for some similar molecules.

Introduction

We have been interested in the conformational stability and/or barriers of internal rotation of organoamine molecules of general formula RNH_2 where R is CH_3CH_2-,[1] $(CH_3)_2-$,[2] $(CH_3)_2CH-$,[3] c-C_3H_5-,[4,5] c-C_4H_7-,[6] $CH_3CH_2CH_2-$,[7] c-C_3H_5-CH_2-,[8] and substituted hydrazines.[9−16] For hydrazine, N_2H_4,[9−11] and tetramethylhydrazine, $N_2(CH_3)_4$,[15] only the gauche conformer is stable whereas for tetrafluorohydrazine, N_2F_4,[16] both the gauche and trans conformers are present in the fluid phases at ambient temperature with an enthalpy difference of 69 ± 6 cm^{-1} (0.83 ± 0.07 kJ/mol). This value of the enthalpy difference was obtained from variable-temperature FT-IR spectra of xenon solutions of N_2F_4. Since hydrazine and the methyl-substituted hydrazines with one, two, or three methyl groups have hydrogen bonding in the liquid state, there are little data available on the conformational enthalpy differences for the methyl hydrazines which have more than one conformer present in the fluid phases at ambient temperature. Therefore as a continuation of our conformational studies of substituted hydrazine molecules, we have investigated the temperature dependence of the vibrational spectrum of methylhydrazine.

There have been several conformational studies[12,17−22] of methyl hydrazine, and it is clear that the *inner* conformer (methyl group between the two hydrogen atoms of the NH_2 group) is more stable than the *outer* form. Thus our interest was to determine the enthalpy difference between the inner and outer forms as well as obtain information on the hydrogen bonding. Therefore, we recorded the variable-temperature FT-IR spectra of xenon solutions of methyl hydrazine. Additionally we have carried out ab initio calculations utilizing the 6-31G(d) basis set at the level of restricted Hartree−Fock and/or with full electron correlation by the perturbation method to second order to determine the optimized structural parameters, harmonic force constants, vibrational frequencies, infrared intensities, Raman activities, and conformational stabilities. We have also calculated the structural parameters and conformational stabilities utilizing the larger 6-311+G(d,p) and 6-311+G(2d,2p) basis sets at the MP2 level as well as density functional theory (DFT) calculations with all three of the basis sets. The results of this spectroscopic and theoretical study are reported herein.

Experimental Section

The sample of methylhydrazine was obtained commercially and distilled at its normal boiling point (86−88 °C). The sample was further purified with a low-temperature, low-pressure fractionating column. The purity of the sample was checked by comparing the mid-infrared spectrum of the vapor to that previously published.[17]

The mid-infrared spectra of the sample dissolved in liquefied xenon as a function of temperature (Figure 1A) were recorded on a Bruker model IFS-66 Fourier transform spectrometer equipped with a globar source, a Ge/KBr beam splitter, and a DTGS detector. The temperature studies ranged from −55 to

[†] Part of the special issue "Mitsuo Tasumi Festschrift".

* Corresponding author. Phone: 01 816-235-6038. Fax: 01 816-235-5502. E-mail: durigj@umkc.edu.

[‡] Taken in part from the thesis of C.Z., which will be submitted to the Department of Chemistry of the University of Missouri−Kansas City, Kansas City, MO, in partial fulfillment of the Ph.D. degree.

[§] University of Missouri−Kansas City.

[||] University of Guyana.

10.1021/jp012244r CCC: $22.00
Published on Web 01/29/2002

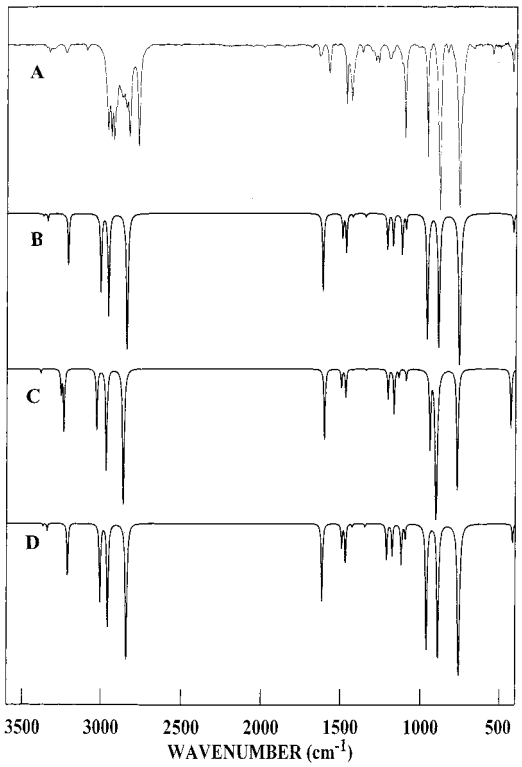

Figure 1. Comparison of experimental and calculated infrared spectra of methylhydrazine: (A) observed infrared spectrum of methylhydrazine in liquid xenon; (B) simulated infrared spectrum of mixture of inner and outer conformers with $\Delta H = 363$ cm^{-1}; (C) simulated infrared spectrum of pure outer conformer; (D) simulated infrared spectrum of pure inner conformer.

−100 °C and were performed in a specially designed cryostat cell consisting of a 4 cm path length copper cell with wedged silicon windows sealed to the cell with indium gaskets. The complete system is attached to a pressure manifold to allow for the filling and evacuation of the cell. The cell is cooled by boiling liquid nitrogen, and the temperature is monitored by two Pt thermoresistors. Once the cell is cooled to a designated temperature, a small amount of sample is condensed into the cell. The system is then pressurized with the rare gas, which immediately starts to condense, allowing the compound to dissolve. For each temperature investigated, 100 interferograms were recorded at a 1.0 cm^{-1} resolution, averaged, and transformed with a boxcar truncation function. All of the observed fundamental bands for the inner conformer and several of those for the outer conformer are listed in Table 1.

Ab Initio Calculations

The LCAO−MO−SCF restricted Hartree−Fock calculations were performed with the Gaussian-98 program[23] using Gaussian-type basis functions. The energy minima with respect to the nuclear coordinates were obtained by the simultaneous relaxation of all the geometric parameters using the gradient method of Pulay.[24] Calculations were also carried out with full electron correlation by the perturbation method[25] to second order up to the 6-311+(2d,2p) basis set. In addition, density functional theory (DFT) calculations made with the Gaussian 98 program[23] were restricted to the hybrid B3LYP method. The determined energy difference that resulted from these various calculations are listed in Table 2 and range from 181 cm^{-1} (2.17 kJ/mol) from the RHF/6-31G(d) calculation to 365 cm^{-1} (4.37 kJ/mol) from the MP2/6-31G(d) calculation with the inner conformer always the more stable form. Most of the other calculations

TABLE 1: Observed and Calculated Frequencies for Inner and Outer Methylhydrazine

		inner						outer						
	fundamental	ab initio[a]	fixed scale[b]	IR int[c]	Raman act.[d]	dp ratio	obsd[e]	PED[f]	ab initio[a]	fixed scale[b]	IR int[c]	Raman act.[d]	dp ratio	obsd[e]	PED[f]
ν_1	NH_2 antisym stretch	3590	3367	0.6	43.0	0.64	335 8	$76S_1$, $19S_3$	3605	3382	0.9	76.9	0.58		$85S_1$, $15S_3$
ν_2	NH stretch	3560	3340	1.6	97.6	0.29	333 9	$95S_2$	3469	3254	5.5	113. 4	0.10		$88S_2$, $11S_3$
ν_3	NH_2 sym stretch	3421	3210	13.4	91.5	0.13	323 5	$80S_3$, $19S_1$	3449	3236	16.9	91.9	0.38		$74S_3$, $14S_1$, $12S_2$
ν_4	CH_3 antisym stretch	3202	3004	23.2	69.5	0.73	296 8	$80S_4$, $20S_5$	3227	3027	16.4	62.8	0.69		$53S_4$, $44S_5$
ν_5	CH_3 antisym stretch	3151	2956	35.9	75.5	0.30	293 0	$55S_5$, $33S_6$, $12S_4$	3163	2967	35.3	76.3	0.37		$31S_5$, $42S_4$, $27S_6$
ν_6	CH_3 sym stretch	3027	2840	68.5	100. 8	0.11	283 5	$67S_6$, $25S_5$	3049	2860	68.9	102. 0	0.11		$69S_6$, $25S_5$
ν_7	NH_2 deformation	1742	1615	22.8	12.3	0.59	158 5	$97S_7$	1727	1602	20.2	12.6	0.59		$97S_7$
ν_8	CH_3 antisym deformation	1577	1492	5.5	16.5	0.75	147 5	$87S_8$	1580	1496	4.2	18.1	0.75		$87S_8$
ν_9	CH_3 antisym deformation	1549	1469	9.4	19.6	0.74	144 2	$91S_9$	1549	1469	6.6	21.6	0.73		$85S_9$
ν_{10}	CH_3 sym deformation	1540	1427	0.7	9.1	0.70	143 0	$92S_{10}$	1529	1424	0.3	7.5	0.73		$87S_{10}$
ν_{11}	NH bend	1503	1346	0.8	5.5	0.74	137 6	$83S_{11}$	1501	1341	0.3	6.5	0.59		$81S_{11}$
ν_{12}	NH_2 twist	1362	1211	8.6	2.1	0.75	121 0	$35S_{12}$, $18S_{15}$, $11S_{13}$	1361	1205	7.1	6.0	0.46		$57S_{12}$, $17S_{14}$, $12S_{13}$
ν_{13}	CH_3 rock	1279	1176	7.6	2.6	0.52	118 4	$33S_{13}$, $28S_{12}$	1263	1137	1.8	5.4	0.31		$41S_{13}$, $31S_{14}$
ν_{14}	CNN antisym stretch	1185	1120	10.0	3.8	0.75	112 9	$88S_{14}$	1214	1091	2.5	8.7	0.75		$15S_{14}$, $34S_{12}$, $29S_{15}$, $13S_{13}$
ν_{15}	CH_3 rock	1178	1095	3.2	8.3	0.75	110 9	$48S_{15}$, $28S_{12}$, $11S_{13}$	1178	1067	11.3	4.3	0.65		$36S_{15}$, $23S_{14}$, $11S_{16}$
ν_{16}	NH_2 wag	1057	962	54.8	4.7	0.68	968	$42S_{16}$, $24S_{13}$, $19S_{17}$	1022	903	121. 4	3.0	0.49	899	$44S_{16}$, $16S_{18}$, $11S_{15}$
ν_{17}	CNN sym stretch	980	890	65.6	5.3	0.34	890	$31S_{17}$, $34S_{16}$, $17S_{18}$	1000	942	23.2	6.5	0.40	948	$61S_{17}$, $19S_{16}$
ν_{18}	NH bend	840	760	120. 2	5.5	0.32	767	$38S_{18}$, $33S_{17}$, $16S_{19}$	852	771	49.6	5.4	0.60		$35S_{18}$, $26S_{17}$, $18S_{16}$, $10S_{19}$
ν_{19}	CNN bend	441	418	4.2	0.7	0.51	428	$60S_{19}$, $29S_{18}$	459	431	15.9	1.1	0.62	440	$63S_{19}$, $20S_{18}$
ν_{20}	NH_2 torsion	362	316	35.4	2.5	0.71	315	$81S_{20}$, $10S_{21}$	292	254	45.4	2.3	0.71	256	$83S_{20}$, $11S_{21}$
ν_{21}	CH_3 torsion	292	275	9.1	0.6	0.72	281	$86S_{21}$, $12S_{20}$	277	263	7.0	0.5	0.74	271	$84S_{21}$

[a] Calculated with the MP2/6-31G(d) basis set. [b] Scaled ab initio calculations with factor 0.88 for stretches, 0.90 for bends except the ∠CNH and ∠NNH 0.75, 0.75 for amino torsion, and 0.90 for methyl torsion. [c] Calculated infrared intensities in km/mol. [d] Calculated Raman activities in Å^4/amu. [e] Values from infrared spectrum of the gas. [f] Values less than 10% are omitted.

TABLE 2: Calculated Energies and Energy Difference for the Two Conformations of Methylhydrazine by ab Initio and Hybrid DFT Methods

		energy diff[a] (c m^{-1})		
method/basis	energy (E_h): inner form	outer form	methyl rotational barrier (V_3 inner)	methyl rotational barrier (V_3 outer)
RHF/6-31G(d)	−150.201 084	181	1320	1444
MP2(full)/6-31G(d)	−150.671 358	363	1345	1334
MP2(full)/6-311+G(d,p)	−150.838 407	238	1340	1248
MP2(full)/6-311+G(2d,2p)	−150.883 192	244	1281	1206
B3LYP/6-31G(d)	−151.170 424	257	1406	1517
B3LYP/6-311+G(d,p)	−151.229 521	272	1171	1076
B3LYP/6-311+G(2d,2p)	−151.235 985	286	1145	1047

[a] Energies of conformations relative to the more stable inner rotamer.

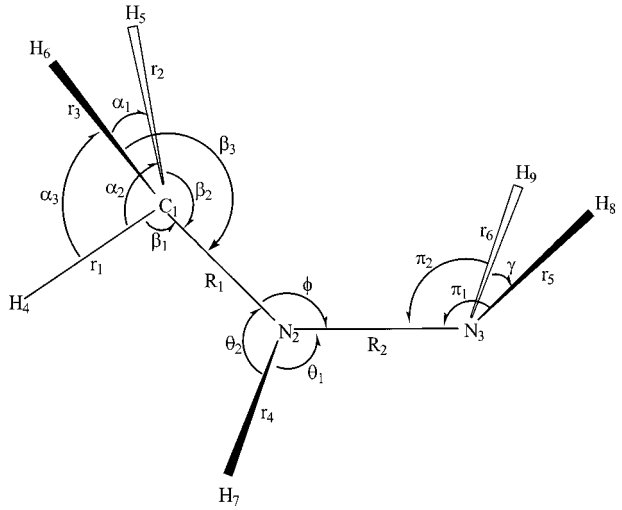

Figure 2. Internal coordinates of methylhydrazine.

gave a value around 250 cm^{-1} always with the inner form as the more stable conformer. The determined structural parameters are listed in Table 1S (Supporting Information).

In order to obtain a complete description of the molecular motions involved in the normal modes of methylhydrazine, a normal coordinate analysis has been carried out. The force field in Cartesian coordinates was obtained with the Gaussian 98 program[23] from the MP2/6-31G(d) calculation. The internal coordinates shown in Figure 2 were used to form the symmetry coordinates listed in Table 3. The *B*-matrix elements[26] were used to convert the ab initio force field from Cartesian coordinates into the force field in desired internal coordinate. The resulting force fields after scaling for both the inner and outer conformers are listed in Tables 2S and 3S, respectively. These force constants were used in a mass weighted Cartesian coordinate calculation to reproduce the ab initio vibrational frequencies and to determine the potential energy distributions (PED) for both conformers which are given in Table 1. The diagonal elements of the force field in internal coordinates were then modified with scaling factors of 0.88 for the CH and NH stretches, 0.9 for the heavy atom stretches, HNH bends, and CH bends, 0.75 for the ∠CNH, ∠NNH, and amino torsion. The geometrical average was utilized for the off-diagonal force constants. The calculation was repeated to obtain the fixed scaled force field and scaled vibrational frequencies.

The infrared and Raman spectra were simulated as shown in Figures 1 and 3, respectively. The frequencies, Raman scattering activities, and infrared intensities were obtained from the output of the ab initio calculations. The Raman scattering cross sections, $\partial\sigma_j/\partial\Omega$, which are proportional to the Raman intensities, can

TABLE 3: Symmetry Coordinates for Methylhydrazine

description	sym coord[a]
NH_2 antisym stretch	$S_1 = r_5 - r_6$
NH stretch	$S_2 = r_4$
NH_2 sym stretch	$S_3 = r_5 + r_6$
CH_3 antisym stretch	$S_4 = 2r_1 - r_2 - r_3$
CH_3 antisym stretch	$S_5 = r_2 - r_3$
CH_3 sym stretch	$S_6 = r_1 + r_2 + r_3$
NH_2 deformation	$S_7 = \gamma - \pi_1 - \pi_2$
CH_3 antisym deformation	$S_8 = 2\alpha_1 - \alpha_2 - \alpha_3$
CH_3 antisym deformation	$S_9 = \alpha_2 - \alpha_3$
CH_3 sym deformation	$S_{10} = \alpha_1 + \alpha_2 + \alpha_3 - \beta_1 - \beta_2 - \beta_3$
NH bend	$S_{11} = \theta_1 - \theta_2$
NH_2 twist	$S_{12} = \pi_1 - \pi_2$
CH_3 rock	$S_{13} = 2\beta_1 - \beta_2 - \beta_3$
CNN antisym stretch	$S_{14} = R_1 - R_2$
CH_3 rock	$S_{15} = \beta_2 - \beta_3$
NH_2 wag	$S_{16} = \gamma + \pi_1 + \pi_2$
CNN sym stretch	$S_{17} = R_1 + R_2$
NH bend	$S_{18} = \phi + \theta_1 + \theta_2$
CNN bend	$S_{19} = 2\phi - \theta_1 - \theta_2$
NH_2 torsion	$S_{20} = \omega$
CH_3 torsion	$S_{21} = \tau$

[a] Not normalized.

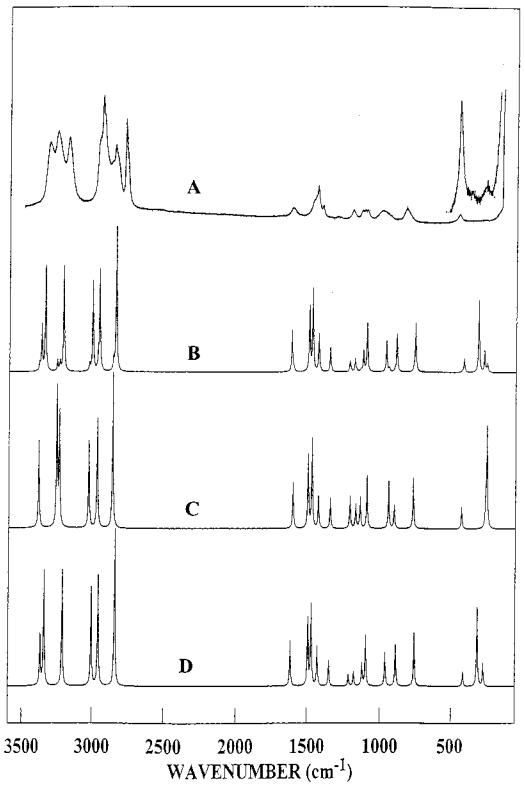

Figure 3. Comparison of experimental and calculated Raman spectra of methylhydrazine: (A) observed Raman spectrum of methylhydrazine in liquid phase; (B) simulated Raman spectrum of of mixture of inner and outer conformers with $\Delta H = 363$ cm^{-1}; (C) simulated Raman spectrum of pure outer conformer; (D) simulated Raman spectrum of pure inner conformer.

be calculated from the scattering activities and the predicted frequencies for each normal mode.[27−30] To obtain the polarized Raman cross sections, the polarizabilities are incorporated into S_j by $S_j[(1-\rho_j)/(1+\rho_j)]$, where ρ_j is the depolarization ratio of the *j*th normal mode. The Raman scattering cross sections and the predicted scaled frequencies were used together with a Lorentzian function to obtain the calculated spectra.

The predicted Raman spectra of the pure inner conformer of CH_3NHNH_2 is shown in Figure 3D, and that of the pure outer

conformer, in Figure 3C. The predicted Raman spectrum of the mixture of the two conformers at 25 °C, with an enthalpy difference of 323 cm^{-1} (value obtained from xenon solution) with the inner conformer the more stable form is shown in Figure 3B. These spectra should be compared with the experimental Raman spectrum of the liquid, shown in Figure 3A, and the simulated Raman spectrum closely resembles the observed spectrum. Although there are some differences in the calculated versus experimental intensities, these data demonstrate the utility of ab initio calculations in predicting the spectrum for conformer identification and vibrational assignments for these types of substituted hydrazine molecules. It should be noted that some of the differences may be the result of hydrogen bonding in the liquid.

The infrared spectra were also predicted from the MP2/6-31G(d) calculations. Infrared intensities were calculated on the basis of the dipole moment derivatives with respect to the Cartesian coordinates. The derivatives were taken from the ab initio calculations transformed to normal coordinates by

$$\left(\frac{\partial \mu_u}{\partial Q_i}\right) = \sum_j \left(\frac{\partial \mu_u}{\partial X_j}\right) L_{ij}$$

where Q_i is the ith normal coordinate, X_j is the jth Cartesian displacement coordinate, and L_{ij} is the transformation matrix between the Cartesian displacement coordinates and normal coordinates. The infrared intensities were then calculated by

$$I_i = \frac{N\pi}{3c^2}\left[\left(\frac{\partial \mu_x}{\partial Q_i}\right)^2 + \left(\frac{\partial \mu_y}{\partial Q_i}\right)^2 + \left(\frac{\partial \mu_z}{\partial Q_i}\right)^2\right]$$

The predicted infrared spectra of the inner and outer conformers are shown in Figure 1D,C, respectively. The mixture of the two conformers is shown in Figure 1B. These spectra can be compared to the experimental spectra of the sample dissolved in liquefied xenon at −75 °C shown in Figure 1A. As a whole, the simulated infrared spectrum closely resembles the observed spectrum, which provides excellent evidence for the quality of the ab initio calculation.

Conformational Stability

To gain information about the enthalpy difference between the two conformers similar to what is expected for the gas, variable-temperature studies in liquefied xenon were carried out. The sample was dissolved in liquefied xenon, and the spectra were recorded at different temperatures varying from −55 to −100 °C. Only small interactions are expected to occur between the dissolved sample and the surrounding noble gas atoms; consequently, only small frequency shifts are anticipated when passing from the gas phase to the liquefied noble gas solutions.[31−35] A significant advantage of this study is that the conformer bands are better resolved in comparison with those in the infrared spectrum of the gas. This is particularly important since most of the conformer bands for this molecule are expected to be observed within a few wavenumbers of each other. Also the areas of the conformer peaks are more accurately determined than those from the spectrum of the gas.

The best separated bands in the infrared spectra of the xenon solution are assigned to the ν_{16} and ν_{17} fundamentals for the two conformers. In Figure 4 the curve fit of the infrared spectrum of methylhydrazine in xenon solution is shown in the 710 to 1050 cm^{-1} region. In Figure 5 is shown the spectral changes for the bands belonging to the two conformers in the infrared spectrum of the xenon solution. The band at 890 cm^{-1} is confidently assigned to the *inner* conformer, and the shoulder at 899 cm^{-1} is due to the *outer* conformer. It is obvious from the weak intensity of the infrared bands assigned to the outer conformer that it is the conformer in the smaller abundance. Additionally there were some bands which increased in intensity as the temperature was lowered, but they were clearly not fundamentals of the inner conformer, i.e., the 745, 838 and 912 cm^{-1} bands (Figure 5). These bands are believed to be due to hydrogen-bonded species where their population increases with decreasing temperature. Therefore, we choose the 899 cm^{-1} band of the outer conformer and the 890 cm^{-1} band for the inner rotamer for the enthalpy determination for the conformational interchange.

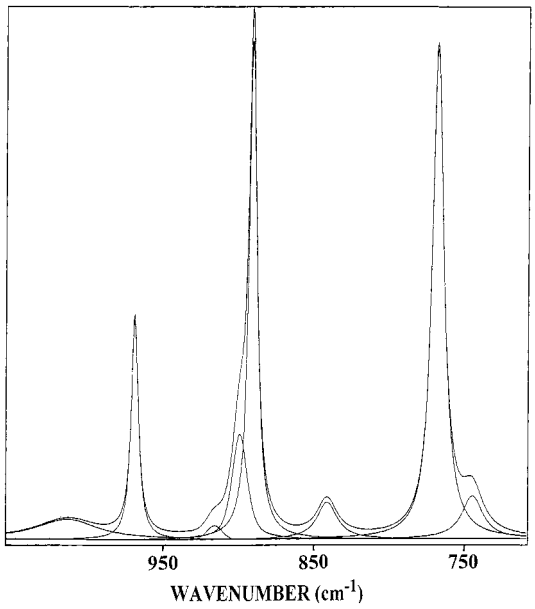

Figure 4. Curve fit of the infrared spectrum of methylhydrazine in xenon solution in the 710−1050 cm^{-1} region.

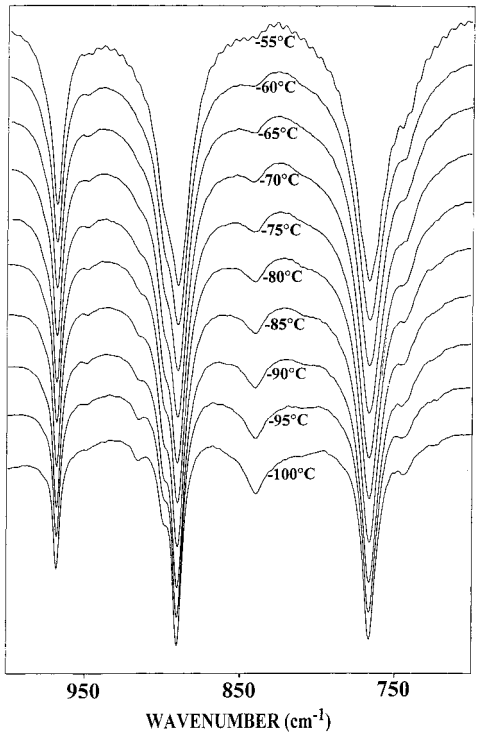

Figure 5. Temperature dependence of infrared bands of methylhydrazine dissolved in liquid xenon.

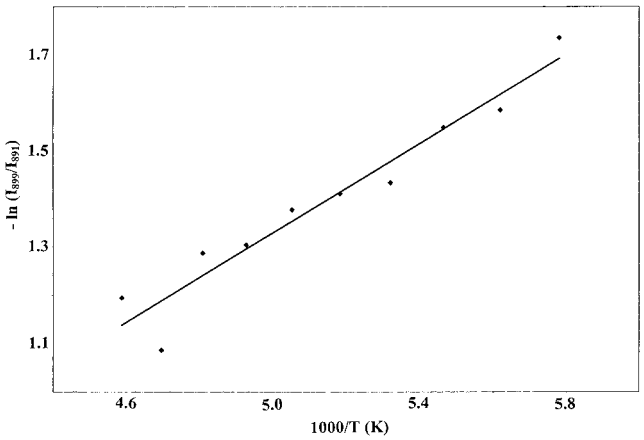

Figure 6. van't Hoff plot of intensity ratios for outer and inner conformer bands of methylhydrazine.

TABLE 4: Temperature and Intensity Ratios from the Conformational and Hydrogen-Bonding Study[a] of Methylhydrazine Dissolved in Liquid Xenon

T (°C)	1000/T (K)	$I_{899/890}$	$I_{745/890}$
−55	4.587	0.3028	0.030 23
−60	4.695	0.3373	0.030 85
−65	4.808	0.2761	0.030 23
−70	4.926	0.2715	0.032 70
−75	5.051	0.2523	0.036 40
−80	5.181	0.2439	0.037 01
−85	5.319	0.2384	0.037 63
−90	5.464	0.2127	0.042 57
−95	5.618	0.2051	0.043 80
−100	5.780	0.1765	0.048 12
ΔH^a		323 ± 30 cm^{-1}	−282 ± 19 cm^{-1}

[a] The enthalpy value of 323 ± 30 cm^{-1} is for the conformational stability and −282 ± 19 cm^{-1} is for hydrogen bond of methylhydrazine.

To obtain the enthalpy difference between the two conformers, 10 spectral data points were obtained over the temperature range of −55 to −100 °C for each conformer band. The intensities of the 899/890 cm^{-1} conformer pair were fit to the following equation: $-\ln K = (\Delta H/RT) - (\Delta S/R)$. The ΔH value was determined from a plot of $-\ln K$ versus $1/T$, where $\Delta H/R$ is the slope of the line and K is the intensity ratio I_i/I_o. It is assumed that ΔH is not a function of temperature over the temperature range.

From the plot (Figure 6) of the natural logarithm of the intensity ratio as a function of the reciprocal of the absolute temperature, an average ΔH value of 323 ± 30 cm^{-1} (3.86 ± 0.36 kJ/mol) was obtained (Table 4) with the inner conformer the more stable rotamer. The error limits are given by the standard deviation of the least squares fit of the intensity data. These error limits do not take into account small associations with the liquefied rare gas or other experimental factors such as the presence of overtones, combination bands, or H-bonded complexes in near coincidence with the measured fundamentals.

Similar data for the intensities of the 745 cm^{-1} band to the 890 cm^{-1} band are also listed in Table 4. The 745 cm^{-1} is believed to be due to a hydrogen-bonded species so we have taken the enthalpy value of −282 ± 19 cm^{-1} for the hydrogen bond.

Vibrational Assignment

The present assignment for the fundamentals of the inner conformer only differs for the assignments for ν_{11} and ν_{13} from those given earlier from the study[17] of the infrared and Raman spectra of CH_3NHNH_2, CD_3NHNH_2, and CD_3NDND_2. In the earlier study[17] ν_{11} was assigned at 1305 cm^{-1} from the Raman spectrum of the liquid (1282 cm^{-1} infrared spectrum of the gas) whereas the ab initio predicted value for this mode is in the range 1346−1426 cm^{-1} depending on the scaling factor of 0.75−0.90 for the NNH angle bend. Therefore the 1376 cm^{-1} band from the xenon solution has been assigned as ν_{11} and the bands at 1293 and 1273 cm^{-1} are believed to arise from either combination bands or from the hydrogen-bonded species (Figure 1A). The ν_{11} fundamental is predicted to be quite weak in the infrared spectrum and relatively weak in the Raman spectrum (Table 1). Previously the ν_{13} fundamental was assigned[17] at 1122 cm^{-1}, which lies between ν_{14} at 1129 cm^{-1} and ν_{15} at 1109 cm^{-1}. However the ab initio predicted value for ν_{13} is 1176 cm^{-1} and there are two choices at 1184 and 1199 cm^{-1}. We have rather arbitrarily chosen the lower frequency band which is weaker than the 1199 cm^{-1} band, mainly because it agrees better with the ab initio predicted value. However if the mixing of this CH_3 rock with the NH_2 twist is less than the predicted amount (Table 1) or the scaling factor is larger than 0.75, then the higher value of 1199 cm^{-1} could be more appropriate.

In the carbon−hydrogen stretching region there appears to be two cases of Fermi resonance. The lower frequency one which involves the CH_3 symmetric stretch at 2777 and 2835 cm^{-1} was reported[17] earlier. However there also appears to be one at 2968 and 2947 cm^{-1} involving one of the CH_3 antisymmetric stretches. The other CH_3 antisymmetric stretch is assigned at 2930 cm^{-1}. These additional two bands in this spectral region (Figure 1A) are too strong to be assigned as arising from the other conformer since it is in only 17% abundance at ambient temperature. However we have assigned a few of the fundamentals, namely ν_{16}, ν_{17}, ν_{19}, and ν_{20}, for the outer conformer on the basis of the ab initio predicted values for these normal modes. It should be noted that ν_{16} has the largest predicted infrared intensity of 121.4 km/mol for the outer conformer.

Discussion

The determination of the enthalpy difference of amines and hydrazines by temperature-dependent infrared spectra of rare gas solutions is complicated by hydrogen bonding of these materials at the low temperature used for these studies. We utilized the CNN symmetric stretch, ν_{17}, at 890 cm^{-1} of the more stable inner conformer and the shoulder at 899 cm^{-1} which has been assigned as the NH_2 wag, ν_{16}, of the outer conformer. This is the fundamental with the highest predicted infrared intensity for this conformer. It was hoped that the CNN symmetric stretch would not be significantly affected by the hydrogen bonding. The enthalpy value of 323 ± 30 cm^{-1} agrees well with the ab initio predicted energy differences which ranged from a low value of 181 cm^{-1} from the RHF/6-31G(d) calculation to a high value 363 cm^{-1} from the MP2/6-31G(d) calculation. The energy difference of 244 cm^{-1} obtained from the MP2/6-311+G(2d,2p) calculation is expected to be the "best" prediction since it is from a calculation with the largest basis set.

The NH bend is predicted at 771 cm^{-1} for the outer conformer, and it is expected to be the second most intense band for this form in the fingerprint region. There is a band at 745 cm^{-1} which might be assigned to this mode. However a van't Hoff plot of the intensity of the 745 cm^{-1} band to the 890 cm^{-1} band of the inner conformer gives a ΔH of −282 ± 19 cm^{-1} (Table 4) with the species giving rise to the 745 cm^{-1} band the more stable form. Therefore, we believe this 745 cm^{-1} band arises from a hydrogen-bonded species and this enthalpy

TABLE 5: Structural Parameters,[a] Rotational Constants, Dipole Moments, and Energies for Methylhydrazine

	MP2/6-311+G(d,p)		microwave[b]		adjusted r_0		electron diffraction[f]	
param	inner	outer	inner	outer	inner	outer	inner	outer
r(C−N)	1.456	1.456	1.44	1.44	1.461	1.461	1.461(12)	1.464(2)
r(N−N)	1.422	1.426	1.45	1.45	1.433	1.437	1.431(12)	1.429(2)
r(C−H_4)	1.093	1.093	1.09[c]	1.09[c]	1.093	1.093	1.095(10)	1.095(10)
r(C−H_5)	1.093	1.091	1.09[c]	1.09[c]	1.093	1.091	1.095(10)	1.095(10)
r(C−H_6)	1.103	1.101	1.09[c]	1.09[c]	1.103	1.101	1.095(10)	1.095(10)
r(N−H_7)	1.013	1.017	1.02[c]	1.02[c]	1.013	1.017	1.011(10)	1.011(10)
r(N−H_8)	1.021	1.013	1.02[c]	1.02[c]	1.021	1.013	1.011(10)	1.011(10)
r(N−H_9)	1.014	1.019	1.02[c]	1.02[c]	1.014	1.019	1.011(10)	1.011(10)
∠(CNN)	113.6	109.5	113	113	113.3	109.3	113.47(21)	109.46(15)
∠(NCH_4)	109.1	108.5	109[c]	109[c]	109.1	108.5		
∠(NCH_5)	109.1	108.6	109[c]	109[c]	109.2	108.6		
∠(H_4CH_5)	108.4	109.1						
∠(NCH_6)	113.2	113.5	109[c]	109[c]	113.3	113.5		
∠(H_4CH_6)	108.7	108.7						
∠(H_5CH_6)	108.3	108.4						
∠(CNH_7)	109.9	109.0	109[c]	109[c]				
∠(NNH_7)	106.4	110.8	109[c]	109[c]	106.4	110.9		
∠(NNH_8)	110.9	108.0	109[c]	109[c]	110.9	108.0		
∠(NNH_9)	107.8	112.0	109[c]	109[c]	107.9	112.1		
∠(H_8NH_9)	107.8	108.5	106[c]	106[c]				
τ(H_4CNN)	−174.3	−178.2			−174.3	−178.2		
τ(H_5CNH_4)	−118.2	−118.4			−118.2	−118.5		
τ(H_6CNH_4)	121.1	121.0			121.2	121.1		
τ(H_7NNC)	−121.1	−120.3			−121.1	−120.4		
τ(H_8NNC)	30.7	−156.1			30.4	−156.8		
τ(H_9NNC)	−87.1	84.5	83.3	83.3	−86.8	83.5		
$\|\mu_a\|$	1.227	0.311	1.04(2)[d]	0.26(3)[d]				
$\|\mu_b\|$	1.420	0.552	1.21(4)[d]	0.60(20)[d]				
$\|\mu_c\|$	0.705	1.950	0.46(9)[d]	1.70(3)[d]				
$\|\mu_t\|$	2.005	2.050	1.66(3)[d]	1.82(5)[d]				
A	37 040	38 480	36704.4(4)[e]	38091.6(3)[e]	36709	38094		
B	9756	9651	9689.89(12)[e]	9591.93(6)[e]	9690	9591		
C	8604	8567	8532.00(11)[e]	8494.42(6)[e]	8533	8497		
$-(E + 150)$	0.838 407	0.837 321						
ΔE (cm^{-1})		238		293(23)				

[a] Bond distances in Å, bond angles in deg, rotational constants in MHz, and dipole moments in D. [b] Reference 18. [c] Assumed parameter. [d] Reference 20. [e] Reference 21. [f] Reference 22.

value is for the hydrogen bond of this NH group in methylhydrazine. The wavenumber for this hydrogen bond in methylamine is 777 cm^{-1} where the NH_2 wag is observed at 785 cm^{-1}.[36] Therefore the difference from the NH bending predicted frequency of 767 cm^{-1} and the hydrogen-bonded band at 745 cm^{-1} is consistent with the observations of the shifts for these modes in methylamine.

Most of the force constant differences for the two conformers are less than 3%, but there are some notable exceptions. The most striking change in value is for r_5 (N−H_8 of NH_2 group), where the value is 8.5% larger for the outer conformer (5.783 verses 6.274 mdyn/Å^2) than the corresponding force constant for the inner conformer. This difference is expected since the N−H_8 bond distance is 0.008 Å shorter in the outer rotamer. The other two N−H stretching force constants have predicted values 5.5% larger in the inner conformer compared to the corresponding ones for the outer conformer (N−H_7, 6.190 verses 5.865 mdyn/Å^2; N−H_9, 6.230 verses 5.895 mdyn/Å^2). Also it should be noted that the force constant for the C−N stretch is 3.6% larger for the outer form (5.028 verses 4.852 mdyn/Å^2) and the NNH_8 bending force constant is 3.9% smaller for the outer conformer (0.724 verses 0.697 mdyn/Å^2), which is consistent with the shorter N−H_8 bond for the outer conformer (Table 5).

These differences lead to some differences in the PEDs for the two conformers. Of particular note are the two CNN stretches where for the inner conformer the antisymmetric stretch, ν_{14}, which is assigned at 1129 cm^{-1} is nearly a pure mode with 88% contribution from S_{14} whereas the corresponding band predicted at 1091 cm^{-1} for the outer conformer has only 15% contribution from S_{14}. The S_{14} symmetry coordinate is predicted to contribute 17%, 31%, and 23% to the predicted fundamentals at 1205, 1137, and 1067 cm^{-1}, respectively, for the outer conformer. The exact opposite differences are predicted for the CNN symmetric stretch, ν_{17}, which is observed at 948 cm^{-1} for the outer conformer with 61% contribution from S_{17} with most of the remaining S_{17} contribution of 26% for ν_{18}, the NH bend. However, for the inner conformer, ν_{17}, which is assigned at 890 cm^{-1}, the S_{17} symmetry coordinate contributes only 31% to this band with contributions of 34% from S_{16} and 17% from S_{18}. There are some significant differences for some of the other modes such as the CH_3 rock at 1184 cm^{-1} for the inner conformer where 33% S_{13} and 28% S_{12} (NH_2 twist) are the major contributions to the PED whereas for the corresponding mode predicted at 1137 cm^{-1} the PED is 41% S_{13} and 31% S_{14} (CNN antisymmetric stretch) for the outer conformer. Nevertheless two-thirds of the modes have 60% or more contribution from the major contributing symmetry coordinate.

By utilization of the different scaling factors of 0.75 (CNH and NNH bends), 0.88 (NH and CH stretches), and 0.90 (CH, HNH, and skeletal bends), the predicted wavenumbers for the fundamentals of the inner conformer have an average error of 13 cm^{-1} which is only 0.8% and considered as an excellent prediction with only three scaling factors. It is possible that the HNH scaling factor should be less than 0.90 since the NH_2 deformation is predicted 30 cm^{-1} higher than the observed value

TABLE 6: Comparison of Rotational Constants Obtained from Modified ab Initio Structural Parameters and Those from Microwave Spectra[a]

		inner			outer		
molecule	rotational consts	obsd	calcd	D	obsd	calcd	D
CH_3NHNH_2	A	36704.40	36703.72	0.68	38091.60	38092.15	−0.55
	B	9689.89	9689.18	0.71	9591.93	9591.04	0.89
	C	8532.00	8531.87	0.13	8494.42	8495.64	−1.22

[a] Values for the rotational constants taken from refs 18 and 21.

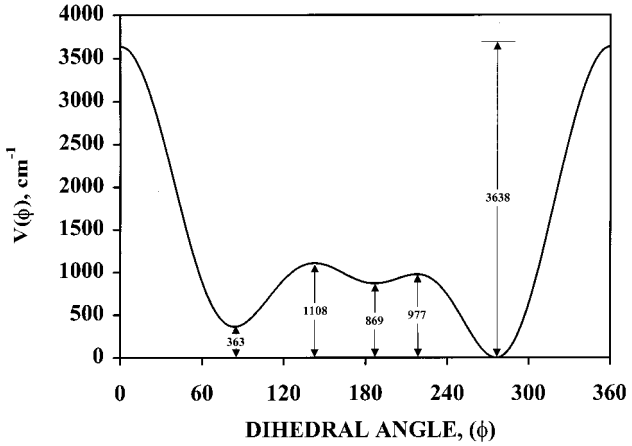

Figure 7. Potential function governing conformational interchange in methylhydrazine.

which is one of the largest errors in the predicted values. However we attempted to use a minimum of scaling factors to give good predicted frequencies. The value of 0.75 for the CNH bending scaling factor was taken from our study of methylamine.[36]

We have calculated the barrier to methyl rotation of the inner conformer by utilizing the 6-31G(d), 6-311+G(d,p), and 6-311+G(2d,2p) basis sets at the level of MP2 with full electron correlation and by density functional theory by B3LYP (Table 2). The values range from a high value of 1406 cm^{-1} to a low value of 1145 cm^{-1} from the B3LYP/6-31G(d) and B3LYP/6-311+G(2d,2p) calculations whereas those from the corresponding MP2 calculations only vary from 1345 to 1281 cm^{-1}. The first reported experimental value[19] of 1338 cm^{-1} was obtained from a reassignment of some earlier reported[17] frequencies taken from a low-resolution far-infrared spectral study. However in a more recently reported[12] low-frequency spectrum of CH_3NDND_2 at a much higher resolution the 1 ← 0 and 2 ← 1 transitions of the inner conformer were assigned at 281.32 and 265.66 cm^{-1}, respectively, which indicates that the earlier assignment of the 1 ← 0 methyl torsion at 262 cm^{-1} was the 2 ← 1 transition. With these more recent torsional assignments for the methyl group the 3-fold barriers of 1602 ± 1 and 1472 ± 19 cm^{-1} were obtained[12] for the inner and outer conformers, respectively. Therefore, the calculated values appear to be low by 200−300 cm^{-1} irrespective of the basis set.

The asymmetric amino torsional potential has been predicted from the ab initio calculations. Beginning at the minimum for the inner conformer a potential function was initially determined by first calculating the energy every 30° with optimization of the structural parameters at each point from the MP2/6-31G(d) calculations. Both the minima and the maxima were determined with optimization, and the resulting potential function is shown in Figure 7. The angle zero is where the methyl group eclipses one of the hydrogen atoms with an energy barrier of 3638 cm^{-1} in going from the inner to the outer form. Additional maxima were obtained at 142 and 217° with a shallow minimum at 187°, which places the lone pair of the nitrogen atom containing the methyl group staggered between the lone pair and a hydrogen atom on the other nitrogen atom, i.e., the other possible staggered conformer. However since the energy difference is so large and the minimum so shallow, one does not expect to see spectroscopic evidence for this form.

This ab initio predicted N−N torsional potential is similar to that obtained from a combination of the microwave and far-infrared spectroscopic data.[19] In this earlier study the cis barrier height of 3028 ± 300 cm^{-1} at an angle of 359° is in excellent agreement with the ab initio value of 3638 cm^{-1} at an angle of 360°. The trans barrier height of 1253 ± 25 cm^{-1} with a maximum at an angle of 197° is similar to the predicted value of 1108 cm^{-1}, which is at 142° but significantly higher than the barrier of 977 cm^{-1} at an angle of 217°. Nevertheless the agreement with the earlier proposed torsional potential[19] is considered quite good.

With utilization of a potential function with five cosine and five sine functions with the form $V = {}^1/_2[\sum_{k=1}^{5} V_k(1 - \cos k\tau) + \sum_{k=1}^{5}(V_k \sin k\tau)]$, the potential constants were obtained. The terms are $V_1 = 1815$, $V_2 = -2047$, $V_3 = 959$, $V_4 = 93$, and $V_5 = -18$ cm^{-1} for the cosine terms with much smaller sine terms of $V_1' = -268$, $V_2' = -9$, $V_3' = 60$, $V_4' = -39$, and $V_5' = -29$ cm^{-1}. These terms were obtained from the MP2/6-31G(d) ab initio predictions and seem reasonable although the V_1 and V_2 terms are somewhat higher than the similar terms for torsional terms governing rotation around C−C bonds.

Recently we have found that MP2/6-311+G(d,p) ab initio calculations give excellent estimates of the CH and CC structural parameters for a large number of monosubstituted hydrocarbons. Therefore, we have carried out a determination of the adjusted r_0 parameters for both conformers of methylhydrazine by using a new program that we developed in this laboratory[37] by combining the previously reported microwave data of the values of the rotational constants for both conformers and the ab initio predicted parameters. This A&M (ab initio & microwave) program fits the rotational constants with the structural parameters remaining close to the ab initio values. To reduce the number of independent variables, the structural parameters are separated into sets according to their types. Each set uses only one independent parameter in the optimization, and all structural parameters in one set are adjusted by the same factor. The differences between similar parameters from the ab initio calculation are retained in the final results. Bond lengths in the same set keep their relative ratio in distances, and bond angles and torsional angles in the same set keep their differences in degrees. This assumption is based on the fact that errors from ab initio calculations are systematic.

With utilization of the isolated C−H stretching frequency[38] from the small amount of the CHD_2NHNH_2 impurity in a CD_3NHNH_2 sample, bands were observed at 2963 and 2897 cm^{-1} which give C−H distances of 1.095 and 1.102 Å. These values are in excellent agreement with the ab initio MP2/6-311+G(d,p) predicted values of 1.093 and 1.103 Å, respectively. Therefore, we held these parameters fixed and varied the heavy atom and nitrogen−hydrogen parameters to reproduce the six

rotational constants. Since the hydrogen atom is so light, there was little change in these parameters, but the C−N distance increased by 0.005 Å and the N−N distance by 0.011 Å (Table 5). This increase in C−N distance is consistent with the similar predictions for this parameter for methylamine utilizing the same ab initio calculations.[36] Also we have found the N−N distance for hydrazine from the MP2/6-311+G(d,p) calculations predicts an N−N bond distance too short.[39] The CNN angle was reduced by 0.3°, and with these changes all but one of the rotational constants is fit to better than 0.9 MHz and the other one (C for the outer conformer) is fit to 1.22 MHz (Table 6). It is believed that these adjusted r_0 parameters should be accurate to 0.003 Å for distances, except for possibly N−H distances, and 0.5° for angles. These are significantly smaller uncertainties than those for the parameters reported from the electron diffraction study.[22] In this study the C−N and N−N distances had a stated uncertainty of 0.012 Å for the inner conformer. Also it should be noted that all of the C−H distances were assumed to be equal at 1.095 ± 0.010 Å, where we are reporting a difference of 0.010 Å between the $C-H_5$ and $C-H_7$ distances for this conformer. The N−N distance for the outer conformer is 0.004 Å longer than the corresponding distance for the inner conformer whereas the electron diffraction results give this bond distance as being 0.002 Å shorter for the outer conformer. It is doubtful that the outer conformer would have a shorter N−N distance than that for the more stable inner conformer. The determined CNN angles agree in the two studies, but the uncertainties for these two parameters were ±2.1 and 1.5° for the inner and outer conformers, respectively, from the electron diffraction study.[22]

We carried out density functional theory (DFT) calculations utilizing the 6-31G(d), 6-311+G(d,p), and 6-311+G(2d,2p) basis sets by the B3LYP method to determine the quality of the structural predictions for this type of molecule. In general the predicted parameters from the 6-31G(d) basis set were very similar to those from the MP2/6-31G(d) calculation except the C−H bond distances were predicted to be about 0.003 Å longer. However, this difference was smaller from the 6-311+G(d,p) calculations but increased from the 6-311+G(2d,2p) calculations. The predicted frequencies for the fundamentals were similar to the quality obtained from the MP2/6-31G(d) calculation and would require scaling factors similar to those used with the MP2/6-31G(d) calculation to provide frequency predictions to 1% or better. Therefore, the only advantage of the DFT calculations appeared to be in the shorter time to complete the calculations.

The use of the isolated N−H stretching frequencies to obtain N−H bond lengths similar to the method used for the C−H bond distances is not currently possible since the earlier attempt to obtain the correlation failed.[40] In this study[40] data were taken from the solid state and the plot of N−H frequency with distance was not a straight line. One might expect such a problem since different crystals are expected to have different hydrogen bond strengths which should affect the N−H distances but not affect the N−H frequencies the same amount. Therefore, a study using the isolated N−H frequencies in the gas phase versus N−H distances would be useful in determining more accurately these bond distances assuming the linearity of the data. We hope to begin such studies soon.

Acknowledgment. J.R.D. acknowledges the University of Kansas City Trustees for a Faculty Fellowship award for partial financial support of this research.

Supporting Information Available: Table 1S, listing structural parameters, rotational constants, dipole moments, and energies for methylhydrazine, and Table 2S, listing force constants of the inner conformer of methylhydrazine. This material is available free of charge via the Internet at http://pubs.acs.org.

References and Notes

(1) Durig, J. R.; Li, Y. S. *J. Chem. Phys.* **1975**, *63*, 4110.
(2) Durig, J. R.; Griffin, M. G.; Groner, P. *J. Phys. Chem.* **1977**, *81*, 554.
(3) Durig, J. R.; Guirgis, G. A.; Compton, D. A. C. *J. Phys. Chem.* **1979**, *83*, 1313.
(4) Compton, D. A. C.; Rizzolo, J. J.; Durig, J. R. *J. Phys. Chem.* **1982**, *86*, 3746.
(5) Kalasinsky, V. F.; Durig, J. R. *Spectrochim. Acta* **1988**, *44A*, 1331.
(6) Kalasinsky, V. F.; Guirgis, G. A.; Durig, J. R. *J. Mol. Struct.* **1977**, *39*, 51.
(7) Durig, J. R.; Beshir, W. B.; Godbey, S. E.; Hizer, T. J. *J. Raman Spectrosc.* **1989**, *20*, 311.
(8) Durig, J. R.; Yu, Z.; Shen, S.; Warren, R.; Verma, V. N.; Guirgis, G. A. *J. Mol. Struct.* **2001**, in press.
(9) Durig, J. R.; Bush, S. F.; Mercer, E. E. *J. Chem. Phys.* **1966**, *44*, 4238.
(10) Baglin, F. G.; Bush, S. F.; Durig, J. R. *J. Chem. Phys.* **1967**, *47*, 2104.
(11) Durig, J. R.; Griffin, M. G.; MacNamee, R. W. *J. Raman Spectrosc.* **1975**, *3*, 133.
(12) Durig, J. R.; Lindsay, N. E.; Groner, P. *J. Phys. Chem.* **1989**, *93*, 593.
(13) Hizer, T. F.; Rizzolo, J. J.; Ives, J. L.; Durig, J. R. *Spectrochim. Acta* **1994**, *50A*, 521.
(14) Durig, J. R.; Harris, W. C. *J. Chem. Phys.* **1971**, *55*, 1735.
(15) Durig, J. R.; MacNamee, R. W.; Knight, L. B.; Harris, W. C. *Inorg. Chem.* **1973**, *12*, 804.
(16) Durig, J. R.; Shen, Z. *J. Phys. Chem. A* **1997**, *101*, 5010.
(17) Durig, J. R.; Harris, W. C.; Wertz, D. W. *J. Chem. Phys.* **1969**, *50*, 1449.
(18) Lattimer, R. P.; Harmony, M. D. *J. Chem. Phys.* **1970**, *53*, 4575.
(19) Lattimer, R. P.; Harmony, M. D. *J. Am. Chem. Soc.* **1972**, *94*, 351.
(20) Yamanouchi, K.; Kato, S.; Morokuma, K.; Sugie, M.; Takeo, H.; Mastumura, C.; Kuchitsu, K. *J. Phys. Chem.* **1987**, *91*, 828.
(21) Murase, N.; Yamanouchi, K.; Sugie, M.; Takeo, H.; Matsumura, C.; Hamada, Y.; Tsuboi, M.; Kuchitsu, K. *J. Mol. Struct.* **1989**, *194*, 301.
(22) Murase, N.; Yamanouchi, K.; Egawa, T.; Kuchitsu, K. *J. Mol. Struct.* **1991**, *242*, 409.
(23) Frisch, M. J.; Trucks, G. W.; Schlegel, H. B.; Scuseria, G. E.; Robb, M. A.; Cheeseman, J. R.; Zakrzewski, V. G.; Montgomery, J. A.; Stratmann, R. E.; Burant, J. C.; Dapprich, S.; Millam, J. M.; Daniels, A. D.; Kudin, K. N.; Strain, M. C.; Farkas, O.; Tomasi, J.; Barone, V.; Cossi, M.; Cammi, R.; Mennucci, B.; Pomelli, C.; Adamo, C.; Clifford, S.; Ochterski, J.; Peterson, G. A.; Ayala, P. Y.; Cui, Q.; Morokuma, K.; Malick, D. K.; Rabuck, A. D.; Raghavachari, K.; Foresman, J. B.; Cioslowski, J.; Ortiz, J. V.; Stefanov, B. B.; Liu, G.; Liashenko, A.; Piskorz, P.; Komaromi, I.; Gomperts, R.; Martin, R. L.; Fox, D. J.; Keith, T.; Al-Laham, M. A.; Peng, C. Y.; Nanayakkara, A.; Gonzalez, C.; Challacombe, M.; Gill, P. M. W.; Johnson, B. G.; Chen, W.; Wong, M. W.; Andres, J. L.; Head-Gordon, M.; Replogle, E. S.; Pople, J. A. *Gaussian 98 (Revision A.7)*; Gaussian, Inc.: Pittsburgh, PA, 1998.
(24) Pulay, P. *Mol. Phys.* **1969**, *17*, 197.
(25) Moller, C.; Plesset, M. S. *Phys. Rev.* **1934**, *46*, 618.
(26) Guirgis, G. A.; Zhu, X.; Yu, Z.; Durig, J. R. *J. Phys. Chem. A* **2000**, *104*, 4383.
(27) Frisch, M. J.; Yamaguchi, Y.; Gaw, J. F.; Schaefer, H. F., III; Binkley, J. S. *J. Chem. Phys.* **1986**, *84*, 531.
(28) Amos, R. D. *Chem. Phys. Lett.* **1986**, *124*, 376.
(29) Polavarapu, P. L. *J. Phys. Chem.* **1990**, *94*, 8106.
(30) Chantry, G. W. In *The Raman Effect*; Marcel Dekker Inc.: New York, 1971; Vol. 1, Chapter 2 (Anderson, A., Ed.).
(31) Bulanin, M. O. *J. Mol. Struct.* **1973**, *19*, 59.
(32) van der Veken, B. J.; DeMunck, F. R. *J. Chem. Phys.* **1992**, *97*, 3060.
(33) Bulanin, M. O. *J. Mol. Struct.* **1995**, *347*, 73.
(34) Herrebout, W. A.; van der Veken, B. J.; Wang, A.; Durig, J. R. *J. Phys. Chem.* **1995**, *99*, 578.
(35) Herrebout, W. A.; van der Veken, B. J. *J. Phys. Chem.* **1996**, *100*, 9671.
(36) Durig, J. R.; Zheng, C. *Struct. Chem.* **2001**, *12*, 137.
(37) van der Veken, B. J.; Herrebout, W. A.; Durig, D. T.; Zhao, W.; Durig, J. R. *J. Phys. Chem. A* **1999**, *103*, 1976.
(38) McKean, D. C.; Duncan, J. L.; Batt, L. *Spectrochim. Acta* **1973**, *29A*, 1037.
(39) Durig, J. R.; Zheng, C. To be published.
(40) Evans, D. F.; Missen, P. H.; Upton, M. W. *J. Mol. Struct.* **1982**, *82*, 147.